Progress In Electromagnetics Research Letters, Vol. 105, 95–102, 2022

Design of an Ultra Compact Antenna for Low Frequency Applications

Basil J. Paul[1, *], Shanta Mridula[1], Anju Pradeep[1], and Pezholil Mohanan[2]

Abstract—An ultra-compact antenna for low frequency application is presented. The resonant frequency band of the proposed antenna is centered at 403.5 MHz, employed for medical implant communication service (MICS) band. The proposed antenna is designed and fabricated on a substrate with $\varepsilon_r = 4.4$, $\tan\delta = 0.02$, and thickness $h = 1.6$ mm. The size of the antenna is only 29 mm × 16.5 mm × 1.6 mm, making it very compact for low frequency of operation. The antenna is evolved from a CPW transmission line. During the process of evolution of the proposed antenna, dual-composite right left handed (D-CRLH) behavior is confirmed from the dispersion diagram. The equivalent lumped circuit model for the antenna is also developed, and the D-CRLH behavior is also confirmed from the circuit model.

1. INTRODUCTION

Antenna plays a key role in a communication system, as it is the element that looks into the surrounding for transmitting or receiving information. The size of this unit has a direct impact on the compactness of a device. Numerous techniques are available in order to develop compact antennas. In [1–3], the authors have reported planar composite right/left handed (CRLH) transmission line based compact antennas. In [4], a dual-composite right/left handed (D-CRLH) transmission line loaded antenna has been reported. In [5–7], chip inductors/capacitors are incorporated for achieving compactness with operating frequency in the range of a few GHz.

Antennas for Medical Implant Communication Service (MICS) band operate in the frequency range 401–406 MHz. As the operating frequency decreases, the size of the antenna increases. Thus the challenge for low frequency antenna designers is to develop a compact antenna that can be well integrated in the device. In [8], the authors have presented compact multilayer antennas with vias for MICS band. In [9], a D-CRLH resonator for a low pass filter with wide rejection band, high roll-off, and transmission zeros is presented. In [10], a compact MICS band antenna based on a split ring resonator with meander line elements is presented. In [11], a ring structured antenna with a via forming a planar inverted-F antenna is presented. The major drawback of such low frequency antennas is the presence of multiple layers and the need for vias. In [12], an ultra-compact antenna based on a D-CRLH tranmission line is presented. In [13], a compact spiral antenna is presented for MICS applications. In [14], a low frequency antenna in the range of a few MHz and in [15], a compact antenna in the ISM band are proposed.

This paper presents an ultra-compact low frequency antenna with chip inductors. During the process of deriving the antenna geometry, D-CRLH behavior is confirmed from the dispersion diagram. The lumped circuit model of the antenna is also proposed. From the circuit model, the antenna resembles the characteristics of a dual-composite right/left handed (D-CRLH) transmission line.

Received 21 March 2022, Accepted 8 July 2022, Scheduled 31 July 2022

* Corresponding author: Basil J. Paul (basiljpaul@mace.ac.in).

[1] School of Engineering, Cochin University of Science and Technology (CUSAT), India. [2] Advanced Centre for Atmospheric Radar Research, Cochin University of Science and Technology (CUSAT), India.

2. GEOMETRY OF THE ANTENNA

Geometry of the proposed antenna is shown in Fig. 1.

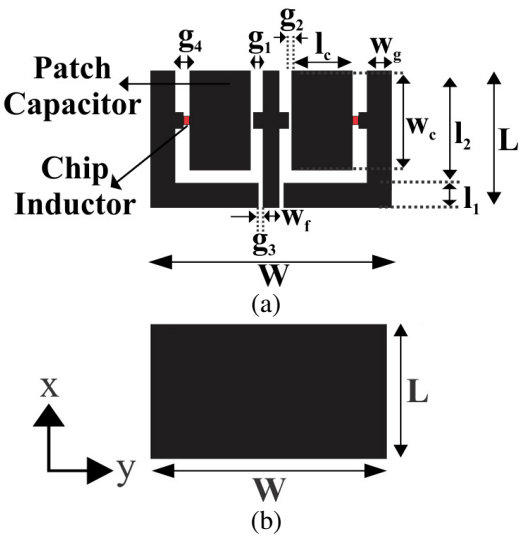

Figure 1. Geometry of the proposed antenna. (a) Top plane. (b) Bottom plane.

It consists of a chip inductor and a distributed patch capacitor connected between a signal strip and the extended ground plane of a truncated CPW transmission line. The resonant frequency of the antenna is determined by the inductance of the chip inductor and the capacitance of the patch capacitor. The operating frequency band of the antenna is centered at 403.5 MHz, the frequency used for medical implants communication service band.

The dimensions of the antenna are $W = 29.02\,\text{mm}$, $L = 16.5\,\text{mm}$, $w_g = 3\,\text{mm}$, $w_f = 2\,\text{mm}$, $g_1 = 1.45\,\text{mm}$, $g_2 = 0.3\,\text{mm}$, $g_3 = 0.5\,\text{mm}$, $g_4 = 1.71\,\text{mm}$, $w_c = 12\,\text{mm}$, $l_c = 7.35\,\text{mm}$, $l_1 = 3\,\text{mm}$, $l_2 = 13.5\,\text{mm}$. The chip inductor used is a 72 nH 0603 HP series coil wound surface mount inductor manufactured by Coilcraft. The self resonant frequency of the inductor is 1.9 GHz, and maximum DC resistance is $0.42\,\Omega$. The patch of length l_c can be approximated as a distributed capacitor since its length $l_c < \frac{\lambda_g}{4}$ where λ_g is the guide wavelength at operating frequency. The CPW transmission line is modified to a cross-shaped structure. The dimensions of the cross is optimized for better impedance matching. The bottom plane consists of a conductor backing throughout the length and width of the antenna.

The evolution of the antenna geometry is shown in Fig. 2. A CPW transmission line with extended ground plane and resonant elements is inserted to obtain resonance in the required band, shown in Fig. 2(a). To convert it into an antenna, the transmission line is truncated as shown in Fig. 2(b). The

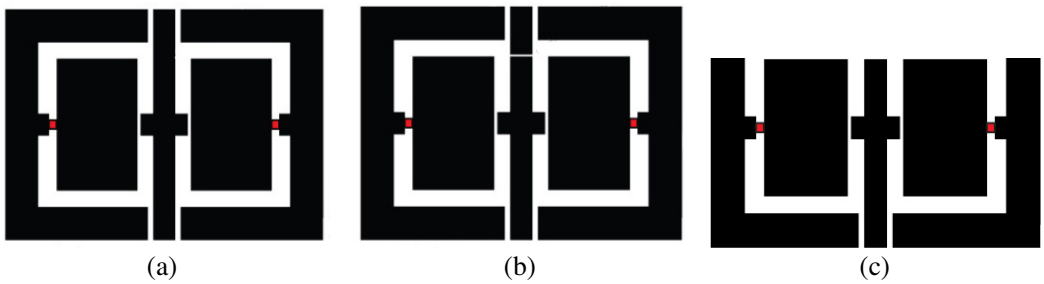

Figure 2. Evolution of the proposed antenna. (a) Extended CPW transmission line with resonant elements. (b) Truncation in transmission line. (c) Proposed antenna geometry.

final antenna geometry is shown in Fig. 2(c). The dispersion characteristic of the truncated transmission line is determined using (1) which relates the propagation constant γ and the scattering parameters [16]. The truncated transmission line with resonant elements inserted shown in Fig. 2(b) is fabricated for the measurement of S_{11} and S_{12}. The measured dispersion characteristic is shown in Fig. 3. Simulated dispersion characteristic is also shown, which is in close agreement with experiment data. The D-CRLH properties of the truncated transmission line can be confirmed by comparing its resonant behavior in the dispersion diagram, shown in Fig. 3, with that of an ideal transmission line.

$$e^{\gamma p} = \left(\frac{1 - S_{11}^2 + S_{21}^2}{2S_{21}} + K \right) \tag{1}$$

$$\text{where} \quad K = \frac{\sqrt{(1 + S_{11}^2 - S_{21}^2)^2 - (2S_{11})^2}}{2S_{21}}$$

The unit cell equivalent circuit and the dispersion diagram of an ideal CRLH and D-CRLH transmission line are shown in Fig. 4 and Fig. 5, respectively. The difference between the dispersion characteristics of CRLH and D-CRLH transmission lines is clear from the slope of the curve marked in the plot by the red line. In the case of CRLH line, the curve has a negative slope initially, followed by a positive sloped region. These indicate left handed (LH) and right handed (RH) regions, respectively [17]. On the other hand for a D-CRLH line, initially the slope is positive followed by a negative sloped region, indicating RH and LH regions, respectively [18–20]. It is clear from the dispersion curve in Fig. 3 that when the transmission line is truncated, it exhibits the behaviour of a D-CRLH transmission line.

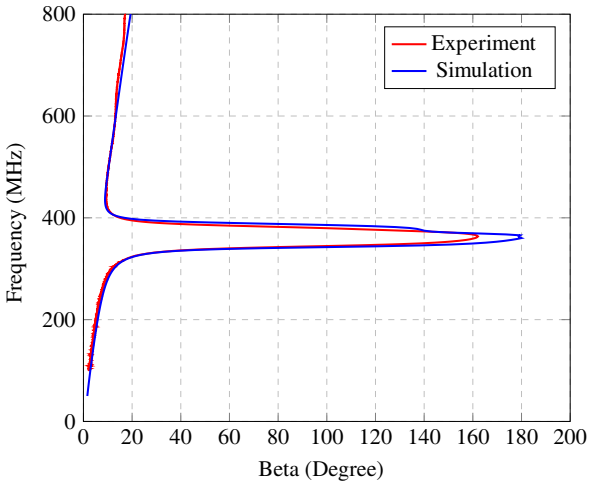

Figure 3. Simulated and experiment dispersion characteristics of the proposed antenna.

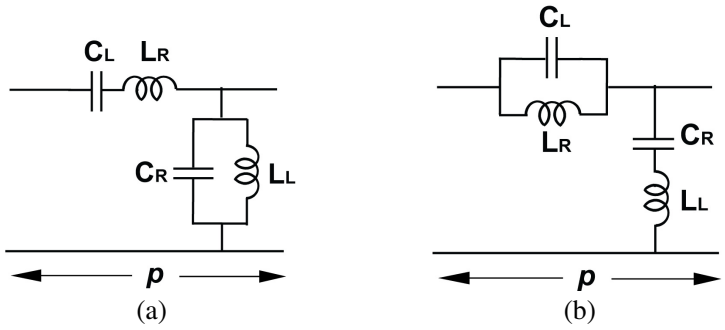

Figure 4. Unit cell equivalent circuit. (a) CRLH transmission line. (b) D-CRLH transmission line.

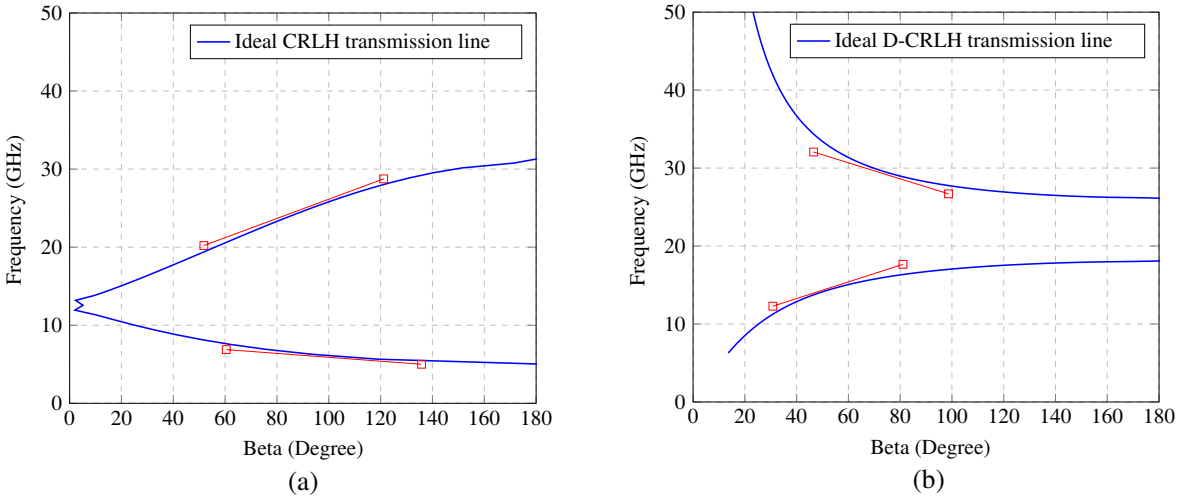

Figure 5. Dispersion diagram of ideal transmission line. (a) CRLH transmission line. (b) D-CRLH transmission line.

3. RESULTS AND DISCUSSION

The proposed antenna is designed and simulated using Ansys HFSS. The antenna is fabricated and tested in the laboratory. A photograph of the fabricated antenna is shown in Fig. 6. The simulated and measured return loss characteristics of the proposed antenna are shown in Fig. 7. Matching at the terminals is obtained by selecting a suitable width of the CPW transmission line and the gap with respect to the CPW ground. The gain of the antenna is measured using 3 antenna method and is found to be −9.49 dBi. The low gain and efficiency of the antenna is due to its compact size at a low operating frequency. The measured radiation patterns of the antenna in y-z and x-z plane are shown in Fig. 8.

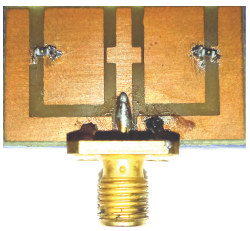

Figure 6. Fabricated prototype of the antenna.

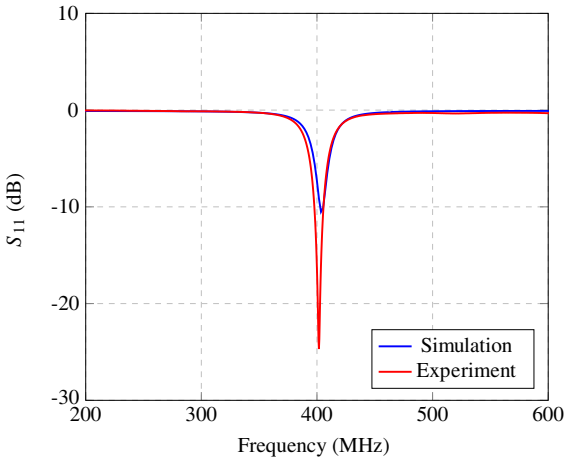

Figure 7. Simulated and measured return loss characteristics of the proposed antenna.

4. LUMPED CIRCUIT MODEL OF THE ANTENNA

A lumped circuit model of the antenna is developed using CST design studio as shown in Fig. 9. The return loss characteristic of the lumped circuit model is shown in Fig. 10.

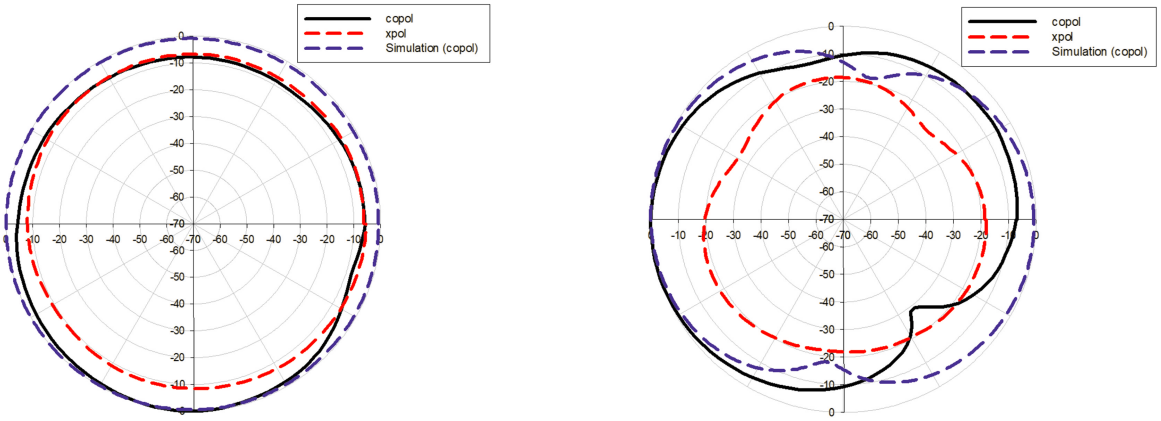

(a) *y*-*z* plane (b) *x*-*z* plane

Figure 8. Measured and simulated radiation pattern of the proposed antenna.

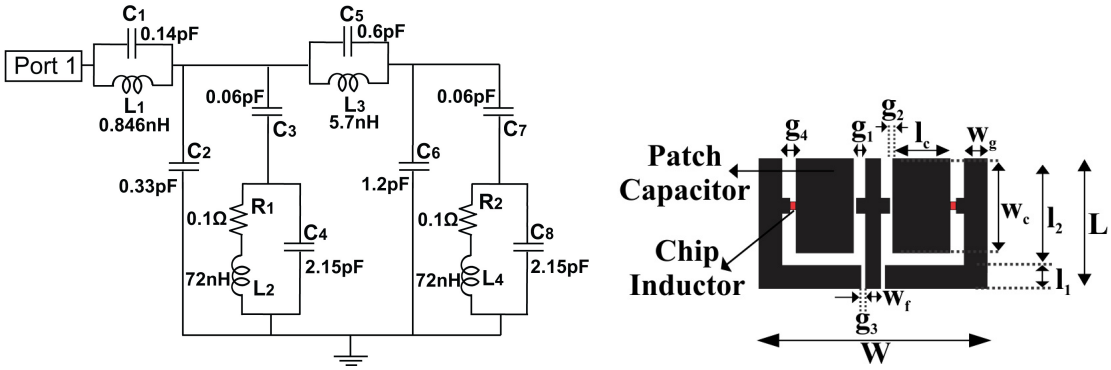

(a) (b)

Figure 9. Lumped circuit model of the antenna.

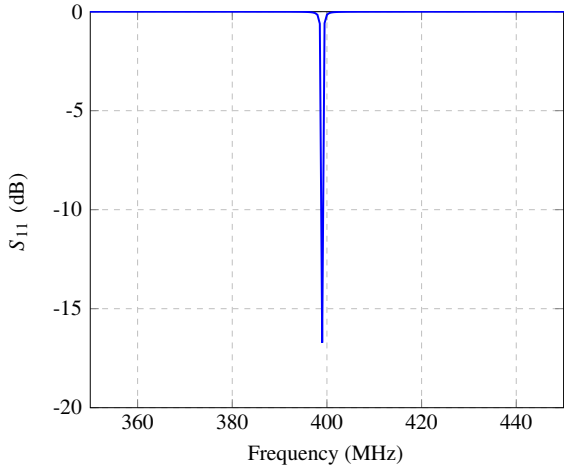

Figure 10. Return loss characteristics of the lumped circuit model.

The per unit length values L_{pul} and C_{pul} of the transmission line feed are found out from the characteristic impedance and phase velocity for each transmission line section of length l_1 and l_2

indicated in Fig. 1.

$$\text{Characteristic impedance, } Z_c = \sqrt{\frac{L_{\text{pul}}}{C_{\text{pul}}}} \tag{2}$$

$$\text{Phase velocity, } V_p = \sqrt{L_{\text{pul}} C_{\text{pul}}} \tag{3}$$

The inductance and capacitance for each transmission line section are found out by multiplying L_{pul} and C_{pul} with the corresponding length of each section [21].

$$\begin{aligned} \text{For section } l_1, \quad & L_1 = L_{\text{pul1}} \times l_1 \\ & C_2 = C_{\text{pul1}} \times l_1 \end{aligned} \tag{4}$$

$$\begin{aligned} \text{For section } l_2, \quad & L_3 = L_{\text{pul2}} \times l_2 \\ & C_6 = C_{\text{pul2}} \times l_2 \end{aligned} \tag{5}$$

C_3 and C_7 are the gap capacitances [22] that exist between the 0.3 mm gap indicated by g_2 in Fig. 1(a).

$$C_3 = C_7 = 0.5C_0 - 0.25C_e \tag{6}$$

where

$$\frac{C_0}{W}(\text{pF/m}) = \left(\frac{\varepsilon_{\text{r}}}{9.6}\right)^{0.8} \left(\frac{s}{W}\right)^{m_0} \exp(k_0) \tag{7}$$

$$\frac{C_e}{W}(\text{pF/m}) = 12\left(\frac{\varepsilon_{\text{r}}}{9.6}\right)^{0.9} \left(\frac{s}{W}\right)^{m_e} \exp(k_e) \tag{8}$$

with

$$m_0 = \frac{W}{h}\left(0.619\log_{10}\left(\frac{W}{h}\right) - 0.3853\right) \tag{9}$$

$$k_0 = 4.26 - 1.453\log_{10}\left(\frac{W}{h}\right) \tag{10}$$

$$m_e = 0.8675; \quad k_e = 2.043\left(\frac{W}{h}\right)^{0.12} \tag{11}$$

C_4 and C_8 represent the parallel plate capacitances that exist between distributed patch capacitor and the bottom conductor backing separated by the substrate.

$$C_4 = C_8 = \frac{\varepsilon A}{d} \tag{12}$$

where A is the area of the distributed patch capacitor, and d is the separation between top plane and bottom plane. L_2 and L_4 indicate the 72 nH chip inductors used in the antenna. The resistances R_1 and R_2 are the coil resistance of the chip inductor. C_1 and C_5 represent the capacitance formed between the transmission line and the bottom conductor plane and is found using (12), where A is the area of the transmission line segment.

5. PERFORMANCE COMPARISON

Table 1 shows the performance comparison of the proposed antenna with other antennas reported in literature. The MICS band antennas proposed in [8, 10, 11] require multiple layers or via process or both, which increases constructional complexity. Additionally, these antennas are designed on substrates with high dielectric constant. In [12], a compact antenna is presented for relatively high frequency applications. In [14], a high gain low frequency antenna is proposed, but it has a drawback of large size. In [15], an ultra-compact antenna at a relatively higher frequency is proposed and is designed on a substrate with high dielectric constant. The proposed antenna is designed on a low cost substrate with low dielectric constant, and it does not require via process to achieve compactness. Moreover, the free space gain of the proposed antenna is better in spite of its compact size.

Table 1. Performance comparison of the proposed antenna.

	Frequency (GHz)	Size (in mm)	Gain (dBi)	Via process	ε_r
Proposed work	0.403	$29.02 \times 16.5 \times 1.6$	-9.49 (free space)	Not required	4.4
[8]	0.403	$16 \times 14 \times 2$	-32	Required	6.7
[10]	0.403	$9.5 \times 9.5 \times 1.27$	-48	Required	10.2
[11]	0.403	$23 \times 16.4 \times 1.27$	-34.9	Required	10.2
[12]	1.57, 2.65	$18 \times 30 \times 1.6$	-	Not Required	4.4
[14]	0.114, 0.221	290×83	1.87, 1.7	Not required	4.3
[15]	2.45	$3 \times 3 \times 0.5$	-24.9	Not required	10.2

6. CONCLUSION

An ultra-compact antenna suitable for low frequency applications is proposed in this paper. The antenna geometry is derived from a truncated CPW transmission line. The compactness of the antenna can be attributed to the resonant elements. The antenna has a simple geometry without any need for a via. During the process of antenna evolution, the D-CRLH behavior of the antenna is confirmed from the dispersion diagram. An equivalent circuit model of the antenna is also developed.

ACKNOWLEDGMENT

The authors would like to thank Kerala State Council for Science Technology and Environment (KSCSTE) for providing financial assistance for this research work as per Council File No. 03/FSHP/2013/CSTE, dated 10/01/2014.

The authors would also like to thank Center for Research in Electromagnetics (CREMA) Laboratory, Dept. of Electronics, Cochin University of Science and Technology, for providing the laboratory facilities.

REFERENCES

1. Park, J.-H., Y.-H. Ryu, J.-G. Lee, and J.-H. Lee, "Epsilon negative zeroth-order resonator antenna," *IEEE Transactions on Antennas and Propagation*, Vol. 55, No. 12, 3710–3712, 2007.
2. Baek, S. and S. Lim, "Miniaturised zeroth-order antenna on spiral slotted ground plane," *Electronics Letters*, Vol. 45, No. 20, 1012–1014, 2009.
3. Pradeep, A., S. Mridula, and P. Mohanan, "Metamaterial based all purpose sensor antenna," *International Journal on Communications Antenna and Propagation*, Vol. 3, No. 3, 181–184, 2013.
4. Li, H.-P., G.-M. Wang, X.-J. Gao, and L. Zhu, "CPW-fed multiband monopole antenna loaded with DCRLH-TL unit cell," *IEEE Antennas and Wireless Propagation Letters*, Vol. 14, 1243–1246, 2015.
5. Luo, Q., J. R. Pereira, and H. M. Salgado, "Compact printed monopole antenna with chip inductor for WLAN," *IEEE Antennas and Wireless Propagation Letters*, Vol. 10, 880–883, 2011.
6. Kim, T. G. and B. Lee, "Metamaterial based compact zeroth-order resonant antenna," *Electronics Letters*, Vol. 45, No. 1, 12–13, 2009.
7. Jee, E. P. and Y. Jee, "Compact dual-band CPW-fed zeroth-order resonant monopole antennas," *IEEE Antennas and Wireless Propagation Letters*, Vol. 11, 712–715, 2012.
8. Garcia-Miquel, A., S. Curto, N. Vidal, J. M. Lopez-Villegas, F. M. Ramos, and P. Prakash, "Multilayered broadband antenna for compact embedded implantable medical devices: Design and characterization," *Progress In Electromagnetics Research*, Vol. 159, 1–13, 2017.

9. Choudhary, D. K., M. A. Abdalla, and R. K. Chaudhary, "Compact D-CRLH resonator for low-pass filter with wide rejection band, high roll-off, and transmission zeros," *International Journal of Microwave and Wireless Technologies*, Vol. 11, 509–516, 2018.
10. Yamac, Y. E. and S. C. Basaran, "A compact dual band implantable antenna based on split-ring resonators with meander line slots," *American Journal of Engineering Research*, Vol. 5, No. 12, 255–258, 2016.
11. Li, R., B. Li, G. Du, X. Sun, and H. Sun, "A compact broadband antenna with dual-resonance for implantable devices," *Micromachines*, Vol. 10, No. 1, 59, 2019.
12. Abdalla, M. A. and A. Fouad, "Integrated filtering antenna based on D-CRLH transmission lines for ultra-compact wireless applications," *Progress In Electromagnetics Research C*, Vol. 66, 29–38, 2016.
13. Palandoken, M., "Compatible bioimplantable MICS and ISM band antenna design for wireless biotelemetry applications," *Radioengineering*, Vol. 26, No. 4, 917–923, 2017.
14. Eldamak, A. R., K. M. Ibrahim, and M. Elkattan, "Implementation of printed small size dual frequency antenna in MHz range," *International Journal of Electronics and Telecommunications*, Vol. 65, No. 4, 565–570, 2019.
15. Yang, F., L. Zhaonan, Q. Lin, S. Wanting, and L. Gaosheng, "A compact and miniaturized implantable antenna for ISM band in wireless cardiac pacemaker system," *Scientific Reports*, Vol. 12, 238, 2022.
16. Eisenstadt, W. R. and Y. Eo, "*S*-parameter-based IC interconnect transmission line characterization," *IEEE Transactions on Components, Hybrids, and Manufacturing Technology*, Vol. 15, No. 4, 483–490, 1992.
17. Caloz, C. and T. Itoh, *Electromagnetic Metamaterials: Transmission Line Theory and Microwave Applications*, John Wiley & Sons, 2006.
18. Caloz, C., "Dual composite right left handed (D-CRLH) transmission line metamaterial," *IEEE Microwave and Wireless Components Letters*, Vol. 16, No. 11, 585–587, 2006.
19. Ryu, Y.-H., J.-H. Park, J.-H. Lee, J.-Y. Kim, and H.-S. Tae, "DGS dual composite right/left handed transmission line," *IEEE Microwave and Wireless Components Letters*, Vol. 18, No. 7, 434–436, 2008.
20. Lu, K., G.-M. Wang, and B. Tian, "Design of dual-band branch-line coupler based on shunt open-circuit DCRLH cells," *Radioengineering*, Vol. 22, No. 2, 618–623, 2013.
21. Paul, B. J., S. Mridula, B. Paul, and P. Mohanan, "Metamaterial inspired CPW fed compact low-pass filter," *Progress In Electromagnetics Research C*, Vol. 57, 173–180, 2015.
22. Hong, J. S. and M. J. Lancaster, *Microstrip Filters for RF/Microwave Applications*, 2nd Edition, John Wiley & Sons, 2001.